uc3m | Universidad Carlos III de Madrid

e-Archivo

This is a postprint version of the following published document:

Alpatov, A., et al. Determination of the force transmitted by an ion thruster plasma plume to an orbital object, In: *Acta astronautica, 119, Feb.-March 2016, Pp. 241-251*

DOI: https://doi.org/10.1016/j.actaastro.2015.11.020

© 2015 IAA. Published by Elsevier Ltd. All rights reserved.

This work is licensed under a Creative Commons Attribution-NonCommercial-NoDerivatives 4.0 International License.

Determination of the Force Transmitted by an Ion Thruster Plasma Plume to an Orbital Object

A. Alpatov[1], F. Cichocki [2], A. Fokov[1], S. Khoroshylov[1], M. Merino[2,c], A. Zakrzhevskii[3]

[1] Institute of Technical Mechanics NAS of Ukraine & SSA of Ukraine, Dnipropetrovsk, Ukraine
[2] Equipo de Propulsión Espacial y Plasmas, Universidad Carlos III de Madrid, Leganés, Spain
[3] S. P.Timoshenko Institute of Mechanics NAS of Ukraine, Kiev, Ukraine
[c] Corresponding autor. email: mario.merino@uc3m.es, telf. +34916248237, fax: N/A

A B S T R A C T

An approach to determine the force transmitted by the plasma plume of an ion thruster to an orbital object immersed in it using its central projection on a selected plane is proposed. A photo camera is used to obtain the image of the object central projection. The algorithms for the calculation of the transmitted force are developed including the determination of the object contour and the correction of the error due to a camera offset from the ion beam axis, and the computation of the fraction of the ion beam that impinges on the object surface.

Keywords: electric propulsion, plasma plume, contactless, space debris, removal, ion beam shepherd

1. Introduction

As a result of space activity, the near-earth Space is littered by a considerable quantity of artificial objects and their fragments, which do not execute useful functions (fragments of final stages of launch vehicles, nonfunctioning spacecraft, etc.). Recent research on the modelling of the population of space debris (SD) shows that the situation for some earth orbits is critical already. For example, results of the official research conducted by the Inter-Agency Space Debris Coordination Committee in 2012, show that the number of SD objects on low earth orbits that will form in the future as a result of collisions will exceed the number of objects that decay and reenter into the atmosphere as a result of natural processes [1]. This fact indicates that the mitigation measures approved by the majority of space nations are insufficient to avoid the continued growth of SD. In view of this, the space community is seriously considering different strategies for active SD removal from earth orbit.

A number of proposed concepts of active removal of orbital fragments are described in the literature, from laser systems [2, 3] to electrodynamic tethers [3, 4]. While docking or grabbing the target object by means of auxiliary devices (for example, a net or a harpoon) is the most obvious means of deorbiting them, this operation may be technologically difficult and unsafe because SD objects are uncontrollable, have a complex motion round the centre of mass, and strongly differ in shape and mechanical properties.

In order to avoid the described complexity, a concept of contactless removal of SD objects named “Ion Beam Shepherd” (IBS) [5] has been proposed. The principle of this concept consists in using a high-velocity jet of ions from a gridded ion thruster (GIT) as a means transmitting momentum to the target object to reposition or force its reentry. The concept of IBS has a number of advantages in comparison with other concepts, namely: efficiency of removal, a low risk level, reusability (multimission) capabilities, and technological readiness.

One of the key problems arising in the research of the IBS concept is the modeling and determination of the force transmitted by the shepherd to the object of SD. Information about this force is necessary both for the successful realisation of the chosen removal program and to solve the navigation and control of the relative motion of the system “Shepherd- SD object.”

Since this problem is relatively new, the amount of publications devoted to it is still small. For example, in [6, 7, 8] the theoretical foundations of the description of the GIT plume and calculations of the transmitted force are proposed. In [9, 10] analytical expressions of the force on a spherical SD object are obtained. Authors of these publications integrate directly the transmitted forces on the object surface. However, application of these results in the form of algorithms onboard the Shepherd is inconvenient due to the required information about the exact shape, size, and orientation of the object. This paper presents an alternative approach that allows determining the transmitted force from far less information about the removed object (target), namely on the basis of its central projection on a chosen auxiliary plane. Such projection can be obtained simply enough by means of a photo camera mounted onboard the Shepherd.

The objective of the present work is to develop the algorithm for the calculation of the force transmitted by the ion beam on a target using its central projection on an auxiliary plane that is perpendicular to the axis of the ion beam, and researching the features of its application to problems of contactless removal of the space debris.

2. Interaction of Ion Beam with Target

The plasma plume of the GIT (ion beam) consists of a flow of heavy ions of propellant (for example, xenon), accelerated to energy levels of a few keV, plus the neutralizing electrons. A rigid body immersed in this plasma jet receives a net force, caused by the momentum of ions bombarding the target. Ions that reach the surface of the target penetrate into its material, lose their momentum and energy to it, and subsequently stop on distance of several nanometers from its surface. After an accommodation time, ions leave the material and escape the target surface at thermal speeds. Since the escaping ion speed is much lower than the incoming ion velocity, this last phenomenon has no essential effect on the transmitted force. Additionally, the energetic ions can have the effect of sputtering the SD material. The contribution to force of these two effects (leaving thermal ions and sputtered materials) can be taken into account as an empirical multiplier factor on the incoming ion momentum; nevertheless, its influence is insignificant on the problem under consideration, and will be neglected hereafter. Likewise, the force caused by electron pressure in the highly hypersonic plasma beam of a GIT is also negligible with respect to the incoming ion momentum in first approximation.

Under these simplifying assumptions, the elementary force transmitted to a differential area of SD object may be calculated as follows [9]:

$$\mathbf{dF} = mn\,\mathbf{U}\left(-\,\mathbf{V}\cdot\mathbf{U}\right)ds\ , \tag{1}$$

where m is the ion mass; n the particle density; $\mathbf{U}$ is the ion velocity vector; ds is the elementary area of surface of the target; $\mathbf{V}$ is the unit normal vector to the elementary area.

The force $\mathbf{F}$ transmitted to the target by the ion beam can be thus calculated as the integral of elementary forces (1) on the irradiated surface of the target S

$$\mathbf{F} = \int_S \mathbf{dF}\ ds\ . \tag{2}$$

3. Ion Beam Model

The plasma plume can be roughly divided into the near (usually less of metre from GIT) and far regions [7, 8]. In the mathematical description of the near region it is necessary to consider influence of the GIT electromagnetic field, cathode emission, and non-uniformity of plasma. For the far region, the influence of these factors becomes insignificant and the distribution of plasma depends essentially on its residual electron pressure and the ambipolar electric field. The beam far region is the region of interest for the problem of contactless removal of the SD considered in this paper, since the plasma and target interaction occurs namely there.

There are many mathematical models having different degrees of complexity and accuracy [8] for the description of the far region of the ion beam. The so-called self-similar model of plasma distribution can be chosen as a compromise model for the purposes of this study.

Self-similar models are based on the supposition that the plasma expansion can be described by means of the dimensionless function of similarity $h(\tilde{z})$ as follows

$$r(z) = r_0 h(\tilde{z}),\ \tilde{z} = z / R_0,$$

where r, z are the radial and axial coordinates of the ion distribution; R_0, r_0 are the initial radius of the beam and the radial coordinate of ion streamlines at an arbitrary initial plane that denotes the the beginning of the far region ($z = 0$).

With use of the function $h(\tilde{z})$, the plasma density at an arbitrary point with coordinates r, z can be determined as follows [8]:

$$n = \frac{n_0}{h^2(\tilde{z})} \exp\left(-C \frac{\tilde{r}^2}{2h^2(\tilde{z})}\right),\ \tilde{r} = r / R_0, \tag{3}$$

where n_0 is plasma density in the beginning of the distant area of the beam; C is a constant defining what part of the plasma flux is contained in the circle of radius R_0 (for example, a value $C = 6$ corresponds to approximately 95 % of the ion current, which is the conventional fraction of plasma current used to define the plume divergence angle, as used below).

The similarity function $h(\tilde{z})$ can be found as the solution of the following differential equation

$$h' = \sqrt{\tan^2 \alpha_0 + \frac{2C}{M_0^2} \ln h},$$

where h' is the derivative of the function $h(\tilde{z})$ with respect to $\tilde{z}$; α_0 is the initial divergence angle of the 95% beam streamtube; and $M_0 = u_0 \Big/ \sqrt{T_e / m}$ is the ion Mach number in the beginning of the distant area; T_e is the electron temperature (here assumed isothermal for simplicity); u_0 is the ion velocity at the origin.

It is necessary to notice that the character of the ion distribution approaches a cone when $M_0 >> 1$, though, strictly speaking, it is not a cone, but a slowly flaring-out tube. For typical values of $M_0 \geq 30$ and distances to the target less than 7 metres, it is safe to asume that the beam is conical with very little error. In this case the similarity function can be approximated as

$$h = \tilde{z} \tan \alpha_0. \tag{4}$$

For the problem under study (highly hypersonic plasma beam), the axial component of the ions velocity does not practically change, and will be assumed constant in the following:

$$u_z = u_{z0} = \text{const}\quad . \tag{5}$$

The radial component of the velocity within the limits of the considered model is defined by following expression [8, 9]:

$$u_r = u_z \tilde{r} \frac{h'}{h}. \tag{6}$$

Taking into account the expression (4) the radial component of the velocity can be represented simply as

$$u_r = u_{z0} \frac{\tilde{r}}{\tilde{z}}. \tag{7}$$

4. Central Projection of the Target

As it has been noted above, under certain conditions the shape of the ion beam can be represented as a cone. Because the plasma properties are different at various angles of the beam, we will divide the cone into finite elements in the spherical coordinates, as it is shown in Fig. 1.

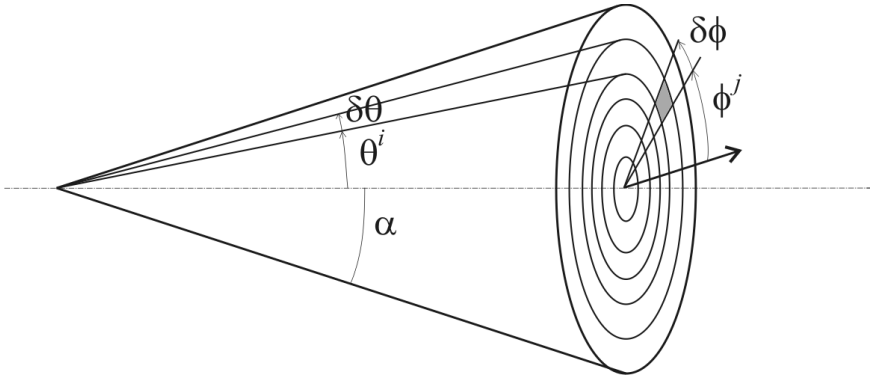

Fig. 1. Partition of ion beam on finite elements

Here θ^i is the discrete polar angle, $\delta\theta$ is the step of the polar descretization, ϕ^j is the discrete azimuthal angle, $\delta\phi$ is the step of the azimuthal discretization.

As the square of the cone cross-section increases proportionally with the distance from the vertex of a cone and the plasma density decreases proportionally to the distance from the virtual vertex (3). Also taking into account the described mechanism of interaction of the beam with the target surface, the elementary force acting on the elementary surface ds of the target is equal to the elementary force acting on a central projection of this surface on some plane that is perpendicular to the axis of the beam. Hence, for the calculation of the force is possible to consider not a 3D target surface but its central projection to a perpendicular plane.

It is obvious that if all rays emanating from the plume vertex hit the target, the force that acts on it is directed along the axis of the beam and is equal to the full GIT thrust. If ions from some area of a ray the $\delta\theta \times \delta\phi$ hit in the target, direction of the acting force coincides with the line of the projection of the centre of this area. Now let us assume that the stream of ions carried by some part of an annular domain hits on the target. Taking into account the conic character of the plasma distribution, there is no necessity to integrate elementary forces all over the target surface; it is enough to sum the resultants of all forces, created by elementary components of the beam, which intersect the central projection of the target to the plane, perpendicular to the beam axis (Fig. 2).

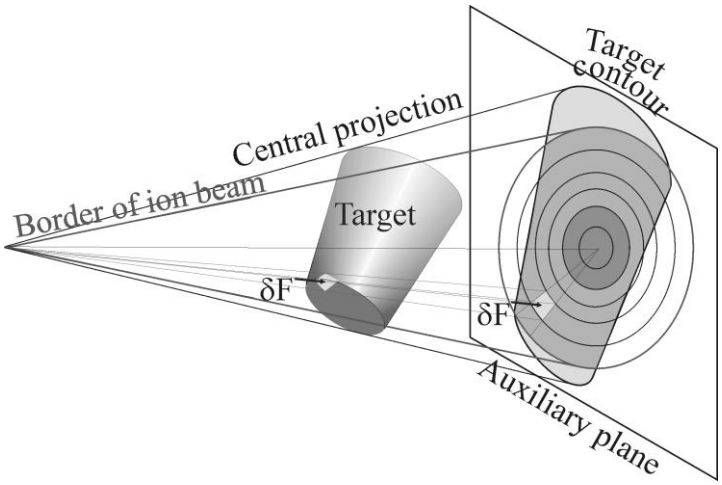

Fig. 2. Central projection of target on auxiliary plane

To continue with the derivation of the force model, we will introduce the following right-handed orthogonal frames of reference.

The frame $O_P x_P y_P z_P$ is fixed to the chosen plane of projection of the beam (FRPL), O_P being the intersection of the plane and the axis of the beam. The axis $O_P z_P$ is perpendicular to plane of projection and is directed toward the target, axes $O_P x_P$ and $O_P y_P$ lie in the projection plane.

The frame $O_T x_T y_T z_T$ whose origin O_T is in vertex of the imaginary cone of the beam is fixed to the GIT (FRE). The axis $O_T z_T$ coincides with the axis of the beam and is directed toward the target. Axes $O_P x_P$ and $O_T x_T$, $O_P y_P$ and $O_T y_T$ are parallel.

The origin of the frame $O_M x_M y_M z_M$ is fixed in the mass centre of the target (FRT). The direction of FRT coincides with the principal central axes of inertia of the target. The attitude of FRT axes with respect to FRE is defined by Euler angles φ , ϑ , ψ .The transitive matrix corresponding to these rotations is

$$T_{MT} = T_\psi T_\varphi T_\vartheta ,$$

where $T_\psi = \begin{bmatrix} \cos\psi & \sin\psi & 0 \\ -\sin\psi & \cos\psi & 0 \\ 0 & 0 & 1 \end{bmatrix}$; $T_\varphi = \begin{bmatrix} 1 & 0 & 0 \\ 0 & \cos\varphi & \sin\varphi \\ 0 & -\sin\varphi & \cos\varphi \end{bmatrix}$; $T_\vartheta = \begin{bmatrix} \cos\vartheta & 0 & -\sin\vartheta \\ 0 & 1 & 0 \\ \sin\vartheta & 0 & \cos\vartheta \end{bmatrix}$;.

Let us approximate the target surface by a mesh of finite surface elements. The mesh here is understood as the topological set of points, connected by edges, segments of straight lines, so that the initial surface is divided into elements of a defined shape. The choice of the partition method depends on the complexity of the target. For example, in case of a cylindrical shape it is enough to set certain amount of points to define the bases of the cylinder. For targets of arbitrary shape methods of triangulation [11] can be used that are well developed and are based on the approximation of surfaces by a mesh of triangles.

The position vectors defining a set of points of the target in FRE can be found as follows:

$$\mathbf{P}_T^l = \mathbf{T}_{MT}\, \mathbf{P}_M^l + \mathbf{B}_{MT} \ , \ l = 1,..., L \ ;$$

where $\mathbf{P}_M^l$ are the vectors defining a set of target points in FRT; $\mathbf{B}_{MT}$ is the vector defining position of FRT origin in FRE; l runs over all points.

Coordinates P_T^l of of the target points, which are projected on the considered plane, are defined as follows:

$$x_P^l = f\,\frac{x_T^l}{z_T^l},\ y_P^l = f\,\frac{y_T^l}{z_T^l}, \tag{8}$$

where f is the distance between points of origins FRPL and FRE; x_T^l, y_T^l, z_T^l are coordinates of points of the target in FRE; x_P^l, y_P^l are coordinates of central projections of points of the target on this plane in FRPL.

5. Evaluation of the Transmitted Force on the Central Projection of the Target

The boundaries of the ring elements of the central projection of a beam (Fig. 1) can be described with the use of the parametrical equation of a circle. The radius of the i -th ring element is defined as follows

$$R^i = f\tan\theta^i,\ 0 \le \theta^i \le \alpha_0,\ i = 1,...,\ I,$$

where I is the number of ring elements.

The angle of a divergence of i -th conic element of the beam can be found as follows:

$$\theta^i = i\delta\theta\ .$$

The set of points that approximate the projection of the mesh of finite elements will be described as:

$$\begin{cases} x_P^{ij} = R^i\cos\phi^j \\ y_P^{ij} = R^i\sin\phi^j \end{cases},\ j = 1,...,\ J,\ 0 \le \phi^j < 2\pi\ . \tag{9}$$

The discrete angle of the parametrical equation of the circle (8) is defined as follows:

$$\phi^j = j\delta\phi\ ,\ j = 0,...,\ J-1,$$

where J is number of sectors in the beam.

As it is seen in Fig. 1, the finite elements defined by three points with coordinates $\left(x_P^0, y_P^0\right)$, $\left(x_P^{1j}, y_P^{1j}\right)$ and $\left(x_P^{j+1}, y_P^{1j+1}\right)$ represent sectors of circles with radius R^1, and the elements characterised by four points with coordinates $\left(x_P^{ij}, y_P^{ij}\right)$, $\left(x_P^{ij}, y_P^{ij}\right)$, $\left(x_P^{i+1j}, y_P^{i+1j}\right)$ and $\left(x_P^{i+1j+1}, y_P^{i+1j+1}\right)$ are truncated sectors. Hence, the area of these elements can be calculated accordingly:

$$ds^{1i} = \left(R^1\right)^2\delta\theta \ \text{ and } \ ds^{i+1j} = \left(\left(R^{i+1}\right)^2 - \left(R^i\right)^2\right)\delta\theta\ ,\ i = 1,...,\ I-1,\ j = 0,...,\ J-1. \tag{10}$$

As mentioned above, the beam can hit on the target only partially. In that case, not all elementary components of the projection of the beam fall within the contour of the target projection and, hence, it is necessary to identify these elements. For this purpose, from the set of all points P_P^l

of the target that are projected on the considered plane, we will first select the K points C_P^l ($k = 1,\ldots, K$) that define a polygon that best approximates the contour of the target projection.

In the case when the target is a convex body, the contour of its projection can be found by solving of the problem of construction of its convex hull, which is fundamental in computational geometry and algorithms for its solution are well developed [11].

For targets of arbitrary shape there are simple and effective algorithms for the construction of nonconvex envelopes characterising the shape of the set of points placed on a plane [12]. The Delaunay triangulation [12] lies at the basis of these algorithms. The shape produced by these algorithms is controlled by a single normalized parameter, which can be used to generate a family of shapes, varying between its convex hull at one extreme and a shape with minimum area. Efficiency of these algorithm is comparable with optimum algorithms for the construction of the convex hulls, namely, the number of evaluations is proportional to $O(n \log n)$, where n is number of input points. Nevertheless, it is necessary to notice that the supposition about convexity of a target allows to use a smaller number of points to approximate its surface, and, hence, to reduce significantly the calculation time.

To identify the elements of the beam projection that are bound by the target contour it is possible to use known algorithms from computational geometry for the point-in-polygon problem [13]. We will consider that an element of the beam is inside the area bounded by the contour if three points of a sector element with the coordinates $\left(x_P^0, y_P^0\right)$, $\left(x_P^{1j}, y_P^{1j}\right)$, $\left(x_P^{1j+1}, y_P^{1j+1}\right)$ or four points of a truncated sector element with the coordinates $\left(x_P^{ij}, y_P^{ij}\right)$, $\left(x_P^{ij+1}, y_P^{ij+1}\right)$, $\left(x_P^{i+1j}, y_P^{i+1j}\right)$, $\left(x_P^{i+1j+1}, y_P^{i+1j+1}\right)$ lie inside the polygon with vertices C_P^k.

With the use of expressions (5) and (7) the velocity vector of ions acting on an elementary area of a target, in FRE, is defined as

$$\mathbf{U}_T^{ij} = \left[u_0 \frac{\hat{x}_T^{ij}}{f}; u_0 \frac{\hat{y}_T^{ij}}{f}; u_0 \right]^T, \tag{11}$$

where $\hat{x}_T^{ij}$, $\hat{y}_T^{ij}$ are the coordinates of the centre of the elementary area in FRE, which are calculated as follows

$$\hat{x}_T^{ij} = \frac{2x_P^0 + x_P^{ijl} + x_P^{ij+1}}{4}, \quad \hat{y}_T^{ij} = \frac{2y_P^0 + y_P^{ij} + y_P^{ij+1}}{4} \quad \forall \quad i = 1,$$

$$\hat{x}_T^{ij} = \frac{x_P^{i-1l} + x_P^{i-1l+1} + x_P^{ijl} + x_P^{ij+1}}{4}, \quad \hat{y}_T^{ij} = \frac{y_P^{i-1l} + y_P^{i-1l+1} + y_P^{ijl} + y_P^{ij+1}}{4} \quad \forall \quad j > 1.$$

After discretizing, the force acting on an elementary area may be defined according to the differential expressions

$$\mathbf{dF}_T^{ij} = mn^{ij} \mathbf{U}_T^{ij} \left(-\mathbf{V}_T^0 \cdot \mathbf{U}_T^{ij}\right) ds^{ij}, \tag{12}$$

$$n^{ij} = \frac{n_0 R_0^2}{f^2 \tan^2 \alpha_0} \exp\left(-C \frac{\left(\hat{x}_T^{ij}\right)^2 + \left(\hat{y}_T^{ij}\right)^2}{2 f^2 \tan^2 \alpha_0} \right), \tag{13}$$

where $\mathbf{V} = [0; 0; -1]^T$ is the unit vector of the normal to the plane, which is perpendicular to the ray.

The force acting on the target is finally calculated as

$$\mathbf{F}_T = \sum_{i=1}^{I} \sum_{j=0}^{J-1} \mathbf{dF}_T^{ij} \,. \tag{14}$$

6. Numerical example

Let us compute the force transmitted by the GIT to a target of cylindrical shape with the proposed approach. The following input data are used for carrying out of the calculations:

The height of the cylinder is h =2.6 m. The diameter of the foundation of the cylinder is d =2.2 m. The target attitude in FRE is the following: $\varphi = 0$ deg, $\vartheta = 45$ deg, $\psi = 45$ deg. The vector defining the position of the mass centre of the target in FRE is: $\mathbf{L}_{ml} = [0 \quad 0 \quad 7]^T$ m. The distance between the centre of projection and the projection plane is f =0.2 m.

Parameters of the GIT are the following: the initial plasma beam radius R_0 = 0.1 m; the ion mass (Xenon) $m = 2.2 \cdot 10^{-25}$ kg; the initial plasma density $n_0 = 2.6 \cdot 10^{16}$ m^{-3}; the initial axial velocity of ions u_0 = 38000 km/s; ion Mach number is assumed infinite to accept the conic approximation for the beam; the angle of the beam divergence $\alpha_0 = 15$ deg.

In Fig. 3 the considered target is shown in FRE. In Fig. 4 the thick line represents a contour of projection of the target on the plane, and the dashed line shows the partition of the ion beam into finite elements.

In Fig. 5 the thicker points note the nodes of the mesh of finite elements of the beam that hit inside the target contour. For the input data introduced above, the vector of the force transmitted to the target calculated with the proposed approach has following components: $\mathbf{F} = [-0.487 \cdot 10^{-4} \quad 0.689 \cdot 10^{-4} \quad 0.07]^T$ N.

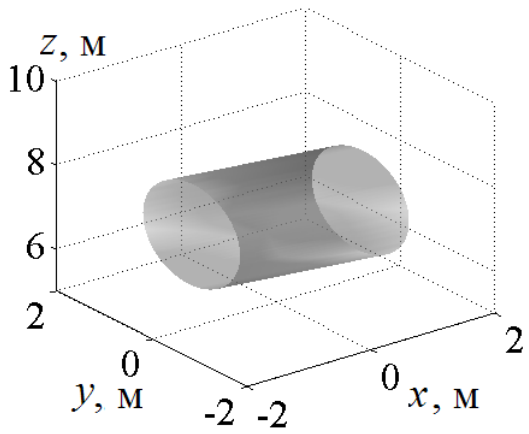

Fig. 3. Target in FRE

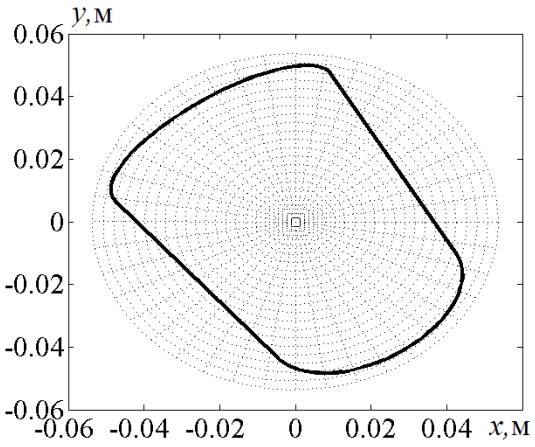

Fig. 4. Contour of central target projection on auxiliary plane

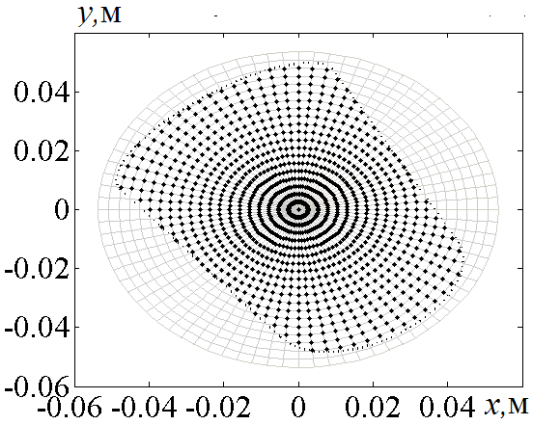

Fig. 5. Nodes of mesh of finite elements of ion beam hitting inside the target contour

7. Determination of Target Contour from Target Imaging

For the determination of the transmitted force, a digital photocamera or similar optical device can be used onboard the Shepherd. The objective of this device is acquiring the central projection of the target. When using photos of the target for the definition of the transmitted force with the above approach it is necessary to determine the coordinates of the points of the contour on its image on a projection plane in FRPL. In the following, additional frames of reference are defined for this purpose.

The frame $O_S x_S y_S z_S$ is connected to the sensitive element of the camera (FRSE), whose origin O_S is fixed in the optical centre of the plane of projection. The axis $O_S z_S$ is perpendicular to the plane of projection and is directed toward the target; axes $O_S x_S$ and $O_S y_S$ are parallel to the central axes of symmetry of the sensitive element. We will consider that the camera is mounted in such a manner that the corresponding axes of frames $O_S x_S y_S z_S$ and $O_P x_P y_P z_P$ are parallel.

The origin O_C of the reference frame connected with the camera (FRC) $O_C x_C y_C z_C$ is arranged on the focal point of the camera. Directions of corresponding axes of FRSE and FRC coincide.

Let us obtain the black-and-white image of a target with transmission of shades of gray (Fig. 6a). We will consider that the camera matrix has N pixels along the abscissa axis and M along the ordinate axis. Then such an image can be described by a matrix G. Each element of this matrix g_{nm} ($n = 1,..., N$; $m = 1,..., M$) can accept a value in the range from 0 to s, where s is the

number of levels of gray. Choosing some threshold value for g_{nm}, we will transform the image G into binary (Fig. 6b) which we will designate as the matrix B. Elements b_{nm} of this matrix can accept values 0 or 1, depending whether g_{nm} is lower or higher than the threshold value. The following step of handling of the image is to identify the pixels from the matrix B which are located on the black and white boundary and form the target contour (Fig. 6c). This contour we will be represented by the matrix C with dimension $K \times 2$, where K is the number of the points forming the contour. Elements of this matrix c_{k1} and c_{k2} are horizontal and vertical indexes of pixel (k-point) of the contour. Thus, contour points are set by indexes of corresponding pixels. Using matrix elements C one can obtain the coordinates of the contour points in FRSE as follows

$$x_S^k = \Delta\left(c_{k1} - n/2\right),\ y_S^k = \Delta\left(c_{k2} - m/2\right), \tag{15}$$

where Δ is size of the pixel of the camera matrix.

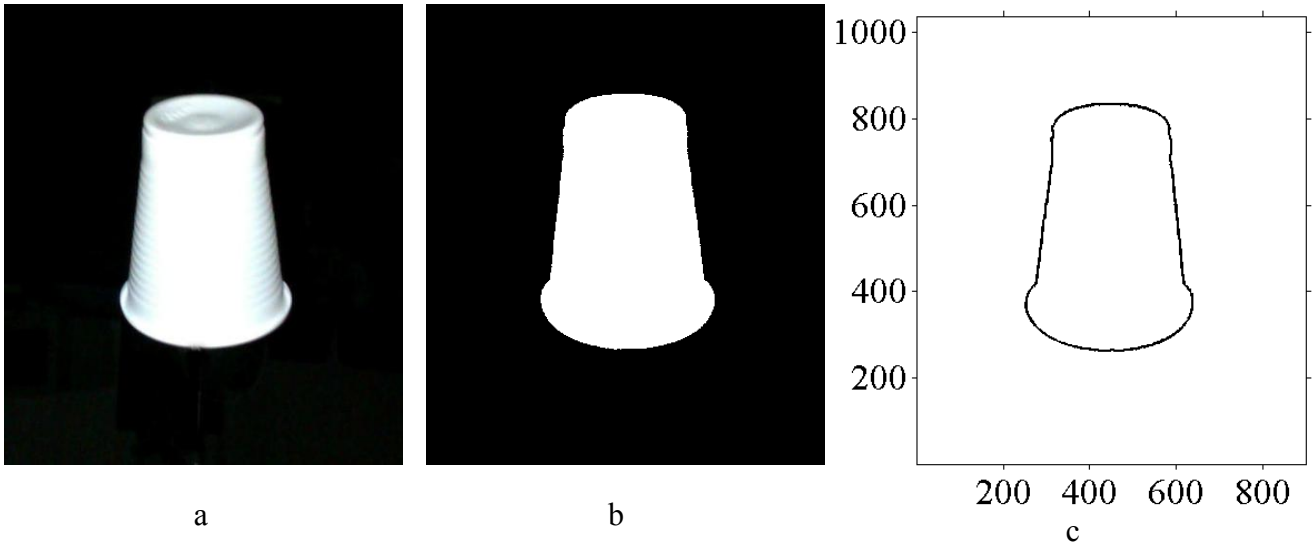

Fig. 6. Digital image processing of target

In a case when the camera is established in such a manner that the focal point of the camera coincides with the vertex of the imaginary cone of the beam, and its focal length is equal to f, frames FRSE and FRPL coincide and expressions (12) define the coordinates of points of the required contour. Here it is necessary to notice that if while choosing the plane of the projection to be placed on a distance equal to the camera focal length is not hard, installing the camera at the vertex of the beam cone is problematic from an engineering point of view. In connection with this, we will consider the case when the camera is positioned with a small shift or offset (0.1 … 0.2 m) relative to the beam axis. Such a shift will cause the contour of the target obtained from the photos to differ from the contour that should be used in the proposed algorithm. This phenomenon is visible in Fig. 7 for the numerical example considered above. Line 1 represents the contour corresponding to a case of coincidence of the focal point of the camera and vertex of the imaginary cone of the beam, and the line 2 shows a contour for the case when the camera is shifted along the axis of ordinates 0.2 m.

Let us consider a possible correction of the coordinates of the points of the contour obtained with use of the expressions (15) to account for this shift. The vectors defining the set of target points in FRC can be found as follows:

$$\mathbf{P}_C^l = \mathbf{P}_T^l + \mathbf{L}_{TC}, \tag{16}$$

where $\mathbf{L}_{TC} = [\tilde{x} \quad \tilde{y} \quad \tilde{z}]^T$ is the vector defining the position of the FRC origin in FRE.

Taking into account expressions (8) and (15), the coordinates of target points projected on the plane of the camera matrix may be defined as follows:

$$x_S^l = f\frac{x_T^l + \tilde{x}}{z_T^i + \tilde{z}},\ y_S^l = f\frac{y_T^l + \tilde{y}}{z_T^i + \tilde{z}}. \tag{17}$$

In view of the fact that it is possible to choose a location for the camera for which $\tilde{z} = 0$, and comparing formulas (8) and (14), it is possible to write the expressions for deriving the coordinates of the points of the contour taking into account the camera offset:

$$x_P^l = x_S^l - \frac{\tilde{x}}{z_T^l},\ y_P^l = y_S^l - \frac{\tilde{y}}{z_T^l}. \tag{18}$$

However, expressions (18) cannot be used directly for the contour correction since it is obviously not possible to define the magnitude of z_T^l for each considered point. Nevertheless, instead of exact values for z_T^l it is possible to use an approximate value. For example, for all points it is possible to use z_0 that is the distance from the vertex of the imaginary cone of the beam to the centre of mass of the target. Taking this into account, expression (18) gives

$$x_P^l = x_P^l - \frac{\tilde{x}}{z_0},\ y_P^l = y_S^l - \frac{\tilde{y}}{z_0}. \tag{19}$$

In Fig. 7a, line 3 represents corrected the contour calculated with use of expressions (18) and using the photo that is obtained by the shifted camera. In this Figure it is visible that the corrected contour practically coincides with the contour obtained by an unshifted camera (line 1).

In Fig. 7b the result of defining the contour of the target by taking into account an inaccuracy in the determination of the position of its center of mass is presented. When carrying out the calculations, it is accepted that the error in the determination of the center of mass represents a random variable with a normal distribution law and zero expectation. The contour 2 is obtained for a mean squared deviation of the error $\sigma = 1$ m, the contour 3 – for $\sigma = 1.5$ m.

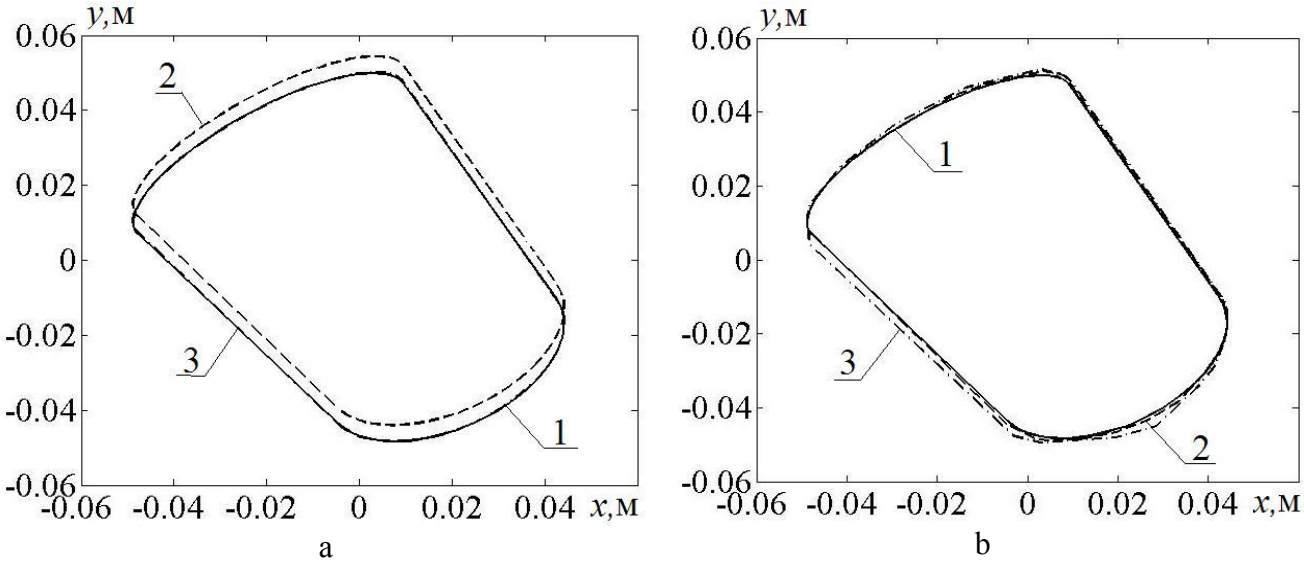

Fig. 7. Contours of target projection

As it can be seen in Fig. 7b, satisfactory outcomes for the determination of the contour of the target are ensured even for a rough determination of the relative position of the centre of mass. Such accuracy in the definition of the position of the center of mass can be ensured by using existing hardware, for example on the basis of remote sensing technology that measures distance by illuminating a target with a laser and analyzing the reflected light (LIDAR).

8. Algorithm for the Calculation of the Transmitted Force

The general algorithm for the calculation of the transmitted force can be summarized into the following steps.

1. Choice of the plane of projection.
2. Partition of the central projection of the GIT beam on finite elements.
3. Definition of the contour of the central projection of the target.
   3. A. For solving the problems of modelling:
      3.A.1. Approximation of the surface of the target by a mesh of finite elements.
      3.A.2. Projection of the central points of the mesh on the chosen plane with use of the expressions (8).
      3.A.3. Calculation of the contour of the target projection on the basis of the solution of the problem of construction of the nonconvex (convex) hull that characterises its projection on the plane.
   3. B. After photos are obtained in orbit:
      3.B.1. Transformation of the initial image to a binary matrix.
      3.B.2. Definition of the pixels forming the contour of the target projection.
      3.B.3. Calculation of the coordinates of the polygon vertices that approximate the contour of the target, with the use of (15).
      3.B.4. Correction of the errors of determination of the target contour due to the shift of the camera with use of the expressions (18).
4. Definition of the finite elements of the ray hitting into the area bound by the contour of the target projection using the solution of the problem of belonging of the central points of an elementary ray to the polygon.
5. Calculation of vectors of the elementary forces for the finite elements selected on the previous step with the use of the formulas (10) - (13).
6. Calculation of the vector of the transmitted force by summation of the elementary forces (14).

9. Conclusion

This paper has been devoted to solving the problem of the determination of the force transmitted by an ion beam to a downstream target in the context of contactless removal of space debris. The approach and algorithms proposed here possess essential advantages in comparison to those that use direct integration of the transmitted forces on the object surface, regarding their need of information about the exact shape, sizes and attitude of the space debris object. In the proposed algorithm, only information on the contour of its central projection on a plane is required. To obtain the image of the target central projection in orbit it is proposed to use a photocamera. Algorithms for the determination of the target contour and identification of the plasma beam elements hitting the target have been developed. Problems of inaccuracy in the determination of the target contour due to a mismatch of the focal point of the camera with the vertex of the imaginary beam cone have been investigated, and algorithms for the correction of the contour defined from the photos of the shifted camera proposed. Numerical calculations illustrating the proposed approach have been carried out. The general algorithm to handle the photos for the determination of the target contour has been presented. Additional work in this area that takes into account real images obtained in orbit that can be a subject of further study.

10. Acknowledgments

The research leading to these results has received funding from the European Union Seventh Framework Programme (FP7/2007-2013) under grant agreement n°607457.

11. References

1. J.-C. Liou, A.K. Anilkumar, B. Bastida at al,Stability of the Future Leo Environment – an IADC Comparison Study, Proc. "6th European Conference on Space Debris" Darmstadt, Germany, 22–25 April 2013 (ESA SP-723, August 2013), 2013.
2. S. Bondarenko, S. Lyagushin, G. Shifrin, Prospects of Using Lasers and Military Space Technology for Space Debris Removal, 2nd European Conference on Space Debris, 1997.
3. C. R. Phipps, J. P. Reilly, ORION: Clearing Near-Earth Space Debris in Two Years Using a 30-kW Repetitively-Pulsed Laser, SPIE Proceedings of the International Society for Optical Engineering, 1997.
4. C. Bombardelli, J. Herrera, A. Iturri, J. Pelaez, Space Debris Removal with Bare Electrodynamic Tethers, Proceedings of the 20th AAS/AIAA Spaceflight Mechanics Meeting, San Diego, CA., 2010.
5. N. Takeichi, Practical Operation Strategy for Deorbit of an Electrodynamic Tethered System. J. of Spacecraft and Rockets. – 2006. – 43. – N 6.–P. 1283–1288. doi:10.2514/1.19635.
6. C. Bombardelli, J. Peláez, Ion Beam Shepherd for Contactless Space Debris Removal, JGCD. – 2011. –34, N 3, May–June, pp. 916–920.
7. F. Cichocki, M. Merino, E. Ahedo, Modeling and Simulation of EP Plasma Plume Expansion into Vacuum, 50th AIAA/ASME/SAE/ASEE Joint Propulsion Conference, 2014.
8. M. Merino, F. Cichocki, E. Ahedo, Collisionless Plasma thruster plume expansion model, Plasma Sources Science and Technology 2015 (currently under review).
9. C. Bombardelli, M. Merino, E. Ahedo, J. Peláez, H. Urrutxua, A. Iturri-Torreay, J. Herrera-Montojoy, Ariadna call for ideas: Active removal of space debris ion beam shepherd for contactless debris removal, Technical report, 2011.
10. C. Bombardelli, H. Urrutxua, M. Merino, E. Ahedo, and J. Peláez, Relative dynamics and control of an ion beam shepherd satellite, Spaceflight mechanics, volume 143 (2012), pp. 2145-2158.
11. P.J. Frey, P.L. George, Mesh Generation Application to Finite Elements / // HERMES Science Europe Ltd, 2000.
M. De Berg, M. Van Kreveld, M. Overmars, O.Schwarzkopf, Computational Geometry: Algorithms and Applications, N.Y.:Springer, 2000.
12. M. Duckham, L. Kulik, M. Worboys, A. Galton, Efficient generation of simple polygons for characterizing the shape of a set of points in the plane, Pattern Recognition, Volume 41, Issue 10, 2008. pp. 2965-3270.
13. K. Hormann, A. Agathos, The point in polygon problem for arbitrary polygons, Comput. Geom. Theory Appl., 20 (2001), pp. 131-144.